Quality Indicator for Ionospheric Biases Interpolation in the Network RTK

Dominik Próchniewicz, Janusz Walo

Department of Geodesy and Geodetic Astronomy
Warsaw University of Technology
Plac Politechniki 1, 00-661 Warsaw

e-mail: d.prochniewicz@gik.pw.edu.pl

Abstract. This paper presents the methodology and performance of an ionospheric quality indicator in the Network RTK. A new index called Zenith Ionospheric Residual Interpolation Uncertainty, which is an extension of the existing indicator is proposed and evaluated using the reference station test network. The dataset used for this study was collected during ionospheric storm period in order to test the indicator during disturbed ionospheric conditions. The test results show that the proposed indicator provides a realistic prediction of ionospheric interpolation accuracy and can be used to predict the Network RTK performance at rover location.

Keywords: Quality Indicator, Network RTK, Ionosphere

1 Introduction

At present the concept of GNSS real-time kinematic positioning using multiple reference station (Network RTK) is the most common approach to relative positioning, which makes it possible to achieve the cm-level accuracy for up to a 50 km baselines (Grejner-Brzezińska *et al.*, 2005; Rizos, 2002). In this approach data from the network of reference stations are used to provides precise measurement corrections, called spatial correction terms, to the user located within the network area. The spatial correction terms, divided into dispersive (ionospheric) and non-dispersive (geometric) part, reduce the distance-dependent errors between the reference station and the user receiver and enable to fix carrier phase ambiguities in near real-time and obtain high accuracy of rover position. In Poland the nation-wide Network RTK service has been provided since 2008 by the ASG-EUPOS network which is a part of European Position Determination System (Bosy *et al.*, 2008).

One of the main factors influencing the accuracy and reliability of Network RTK technique is the precision of determining spatial correction terms. Especially during storm-level ionospheric activity the applied spatial interpolation model may not be suitable for the real ionospheric state, causing the ambiguity resolution to be less reliable or even impossible due to high ionospheric residuals. In this aspect the quality indicator for ionospheric biases interpolation can be a very important tool to provide the performance index of kinematic positioning in real-time.

In recent years several quality indicators for Network RTK techniques have been developed which were based on the observations on additional monitor station (Chen *et al.*, 2003; Wanninger, 2004) or on the measurements of linearity of distance-dependent errors over the network of reference stations (Alves *et al.*, 2005). In this work a different approach using the standard deviation of the interpolation model scaled to zenith will be developed. This allows to determine the quality indicator as a function of baseline length.

2 Ionosphere quality indicator methodology

The main computation steps of the proposed ionosphere quality indicator algorithm can be describe as follows:

- fixing the double-differenced carrier phase ambiguity between reference stations;
- determining the dispersive part of distance-dependent biases between reference stations;
- generating a model of interpolation of the dispersive biases as well as its uncertainty;
- determining the ionosphere elevation mapping function to map the double-differenced ionosphere biases to zenith;

- calculating the cumulate Zenith Ionospheric Residual Interpolation Uncertainty with a confidence level of 95% (ZIRIU95) over all pairs of reference-other satellite for certain epoch and location.

2.1 Distance-dependent biases between reference stations

Double-differenced carrier phase ambiguity resolution (AR) between reference stations is the first step to determining the spatial correlated errors (which will be divided into dispersive and non-dispersive parts). When the coordinates of reference stations are well known and the maximum length of baselines between them are up to 50 km (as in the used reference stations network) the AR can be followed by the wide-lane/narrow-lane $(L5/L3)$ approach (Mervart, 1995; Chen *et al.*, 2000). The "Melbourne-Wübbena" phase-code dual-frequency combination is used in this approach to resolve the wide-lane double-differenced ambiguity at first (Melbourne, 1985; Wübbena, 1985; Hofmann-Wellenhof *et al.*, 2008). For detailed information please refer to Próchniewicz (2011).

In this study, the Kalman filter was used to estimate the float ambiguity and the Least-squares AMBiguity Decorrelation Adjustment (LAMBDA) (Teunissen, 1995) and Modified LAMBDA methods (Chang *et al.*, 2005) were applied to fix ambiguity with the ratio test (more than 3.0) as a threshold of validation. Discontinuities in the double-differenced ionospheric residuals were used to detect and repair the cycle slips.

When the double-differenced integer ambiguity for L_1 and L_2 between reference stations is determined, the double-differenced carrier phase residuals $(\nabla\Delta\bar{\Phi}_k)$ can be obtained as follows:

$$\nabla\Delta\bar{\Phi}_k = \nabla\Delta\Phi_k - \frac{f_k}{c}\left(\nabla\Delta\rho + \nabla\Delta T\right) - \nabla\Delta N_k \qquad (1)$$

where Φ_k is the carrier phase observables for f_k frequency in cycles; ρ is the geometric satellite-to-receiver distance in meters; T is the tropospheric delay in meters and N_k is the integer ambiguity in cycles; $\nabla\Delta$ is the symbol of double-difference. In this study, the double-differenced carrier phase residuals were computed using the Saastamoinen model of tropospheric delay (Saastamoinen, 1973) with standard atmosphere parameters and the Niell mapping function for wet and dry components (Niell, 1996). The double-differenced geometric satellite-to-receiver distances were obtained using final precise ephemerids from the International GNSS Service (IGS) and relative antenna calibrations from the National Geodetic Survey (NGS) (Mader, 1999).

The distance-dependent biases appear as carrier phase residuals and can be separated to dispersive (ionospheric delay) and non-dispersive (geometric) parts using the formulas:

$$\nabla\Delta I_1 = \frac{f_2^2}{f_1^2 - f_2^2}\left(\frac{c}{f_1}\nabla\Delta\bar{\Phi}_1 - \frac{c}{f_2}\nabla\Delta\bar{\Phi}_2\right) \quad (2)$$

$$\nabla\Delta G = \frac{f_1^2}{f_1^2 - f_2^2}\left(\frac{c}{f_1}\nabla\Delta\bar{\Phi}_1 - \frac{cf_2}{f_1^2}\nabla\Delta\bar{\Phi}_2\right) \quad (3)$$

where $\nabla\Delta I_1$ is the double-differenced ionospheric delay for L_1 in meters and $\nabla\Delta G$ is the double-differenced geometric delay in meters reflecting residual tropospheric delay, orbit errors, reference station errors and so on. In this paper the quality indicator for ionospheric bias interpolation is presented only but a similar indicator could be used for non-dispersive parts as well.

2.2 Ionosphere residual interpolation uncertainty

The standard deviation of the interpolation model for dispersive biases can be used as an ionospheric quality indicator (see Chen *et al.*, 2003). The standard deviation represents the congruence of the used interpolation model for ionospheric biases with the real biases. If the used interpolation method is based on linear interpolation then the indicator reflects the ionospheric linearity over the network. This indicator can be calculated epoch-by-epoch for a specific rover location and for all satellite pairs.

In this study, the Weighted Linear Interpolation Method (WLIM) was used to model the ionospheric biases. This method is some variety of the Linear Interpolation Method (LIM) proposed by Wanninger (1995) and extended by Wübbena *et al.* (1996). The WLIM algorithm describes distance-dependent biases as a three parameter plane model, as follows:

$$\nabla\Delta I_{m,u} = \begin{bmatrix}\Delta x_{m,u} & \Delta y_{m,u} & 0\end{bmatrix}\begin{bmatrix}a\\ b\\ c\end{bmatrix} \tag{4}$$

where $\nabla\Delta I_{m,u}$ is the ionospheric correction from the master m to the user u stations and $\Delta x_{i,j}$, $\Delta y_{i,j}$ are the plane coordinates differences between i and j stations. Network coefficients a and b estimates for the north and east gradients of the plane model and c estimates for the constant part represents the station-specific error. At least four reference stations is needed to compute the network coefficients, and at least five to obtain the standard deviation of the interpolation model. Least-square adjustment can be used to estimate the vector of network coefficients $\mathbf{X}$:

$$\mathbf{X} = \left(\mathbf{A}^T\mathbf{P}\mathbf{A}\right)^{-1}\mathbf{A}^T\mathbf{P}\mathbf{R} \tag{5}$$

$$\mathbf{X} = \begin{bmatrix}a\\ b\\ c\end{bmatrix} \qquad \mathbf{A} = \begin{bmatrix}\Delta x_{m,1} & \Delta y_{m,1} & 1\\ \Delta x_{m,2} & \Delta y_{m,2} & 1\\ \vdots & \vdots & \vdots\\ \Delta x_{m,n-1} & \Delta y_{m,n-1} & 1\end{bmatrix} \qquad \mathbf{R} = \begin{bmatrix}\nabla\Delta I_{m,1}\\ \nabla\Delta I_{m,2}\\ \vdots\\ \nabla\Delta I_{m,n-1}\end{bmatrix}$$

where $\mathbf{P}$ is the distance-dependent weighting matrix based on the inverse of distance between the reference station and user station; $\mathbf{R}$ is the observables vector consisting of the ionospheric biases between reference stations (subscripts $1, 2, \ldots, n$ denote the number of reference stations). The corresponding covariance matrix $\mathbf{Q}$ can be obtained using the equations:

$$\sigma_0^2 = \frac{\mathbf{V}^T\mathbf{P}\mathbf{V}}{n-3} \tag{6}$$

$$\mathbf{Q} = \sigma_0^2\left(\mathbf{A}^T\mathbf{P}\mathbf{A}\right)^{-1} \tag{7}$$

where σ_0^2 is the variance of unit weight and $\mathbf{V}$ is the vector of residuals.

The ionospheric quality indicator can be calculated as a standard deviation of the WLIM model σ_r by the equation:

$$\sigma_r = \sqrt{\mathbf{rQr}^T} \tag{8}$$

where $\mathbf{r} = \begin{bmatrix} \Delta x_{m,u} & \Delta y_{m,u} & 0 \end{bmatrix}$ describes the specific rover location for which the indicator is calculated.

2.3 Ionosphere elevation mapping function

In order to calculate the quality indicator as a single value for all reference-other satellite observables, the ionospheric elevation mapping function is needed. This function allows the interpolation errors for current satellite elevation directions (expressed by Equation 8) to be converted to zenith value and the cumulative quality indicator to be obtained.

The general formula for the elevation mapping function, which maps the ionospheric delay at elevation ε (I_ε) on the zenith value I_z can be described:

$$\mu\left(\varepsilon\right) = \frac{I_\varepsilon}{I_z}. \tag{9}$$

The goal of this subsection is to determine a mapping function $\mu_{\nabla\Delta}\left(\varepsilon^a, \varepsilon^b\right)$ that maps the double-differenced ionospheric bias ($\nabla\Delta I_{i,j}^{a,b}$) to the double-differenced ionospheric bias at zenith ($\nabla\Delta I_{i,j}^{a,b} z$). Converting Equation 9 to double-differenced value yields:

$$\mu_{\nabla\Delta}\left(\varepsilon^a, \varepsilon^b\right) = \frac{\nabla\Delta I_{i,j}^{a,b}}{\nabla\Delta I_{i,j}^{a,b} z} \tag{10}$$

where subscripts i and j denote receivers and superscripts a and b denote satellites. Based on the definition of double-differenced observables and assuming that $(I_i^a z - I_j^a z) = (I_i^b z - I_j^b z)$, the double-differenced mapping function can be reduced (Raquet, 1998):

$$\mu_{\nabla\Delta}\left(\varepsilon^a, \varepsilon^b\right) = \frac{\mu\left(\varepsilon^a\right) + \mu\left(\varepsilon^b\right)}{2} \tag{11}$$

where ε^a and ε^a are the average elevations of satellites a and b between receivers i and j .

Defining the variance of double-differenced ionospheric delay as:

$$\sigma^2_{\nabla\Delta I} = E[(\nabla\Delta I)^2] \tag{12}$$

the mapping function of double-differenced variance can be described by expression:

$$\mu^2_{\sigma^2_{\nabla\Delta}}\left(\varepsilon^a, \varepsilon^b\right) = \frac{E[(\nabla\Delta I^{a,b}_{i,j})^2]}{E[(\nabla\Delta I^{a,b}_{i,j} z)^2]} \tag{13}$$

where $E[X]$ is the expected value of X. In Equations 12 and 13 we assumed that $\nabla\Delta I$ is zero-mean and that errors between satellites are uncorrelated (Raquet, 1998). Finally, using the same approach as in Equation 11 the mapping function of double-differenced variance is presented as:

$$\mu^2_{\sigma^2_{\nabla\Delta}}\left(\varepsilon^a, \varepsilon^b\right) = \frac{\mu^2\left(\varepsilon^a\right) + \mu^2\left(\varepsilon^b\right)}{2}. \tag{14}$$

Equations 13 and 14 show that the elevation mapping function $\mu\left(\varepsilon\right)$ can be obtained from the variance of double-differenced ionospheric delay and this approach was used in the analysis of test network data described in Section 3.2.

3 Ionospheric Quality Indicator Performance Using Test Data

3.1 Test data

In order to test how well the proposed ionospheric quality indicator can approximate real interpolation errors the multiple reference stations test network was used. The test network consisted of 14 ASG-EUPOS reference stations was divided into three sub-networks. For each sub-network an independent interpolation model of dispersive biases was created. The reference station KALI was used as a master reference station for all sub-networks and the stations: SIDZ, KONI and KROT were selected as user stations. The ionospheric

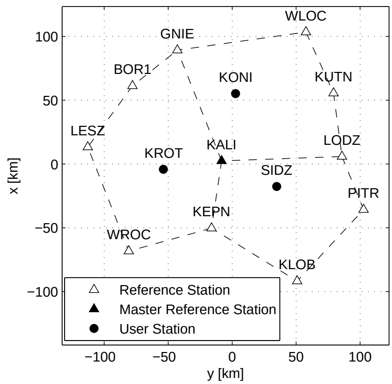

Figure 1. *Reference station test network*

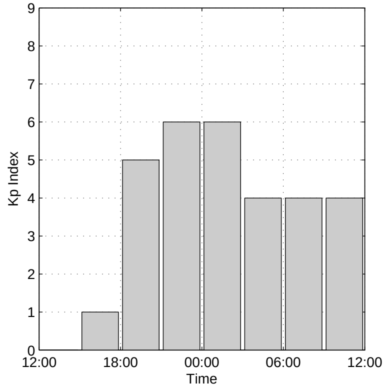

Figure 2. *Estimated Kp index*

biases for master station-user stations baselines were not included in the interpolation algorithm and were used as *true* values to verify the ionospheric quality indicator performance. In Figure 1 the used test network is presented. All calculations presented in this paper were performed using the MATLAB scripts developed by the authors.

The 24-hour GPS dual-frequency phase and code data with 15 seconds sampling rate and 15 degrees elevation cut-off was collected from 4 (12UT) to 5 (12UT) June 2011. During the test the Kp index reached a value of 6 (see Figure 2, source: `www.swpc.noaa.gov`) which indicates storm-level ionospheric activity (for Kp index greater than 5). The Kp index is a measure of global geomagnetic activity computed for 3 hours of data with a maximum value of 9 (Bartels, 1957).

In Figure 3 the double-differenced ionospheric biases (for L_1 in meters) for all satellites (related to the reference satellite) for three user station baselines are presented. Using the WLIM method (see Section 2.2), the predicted double-differenced ionospheric delay (denoted as a *grey line*) and the measurement values of double-differenced ionospheric delay (*black line*) show a good agreement for all baselines during the test period, excluding the ionospheric storm period. For this period, the differences reach more than 10

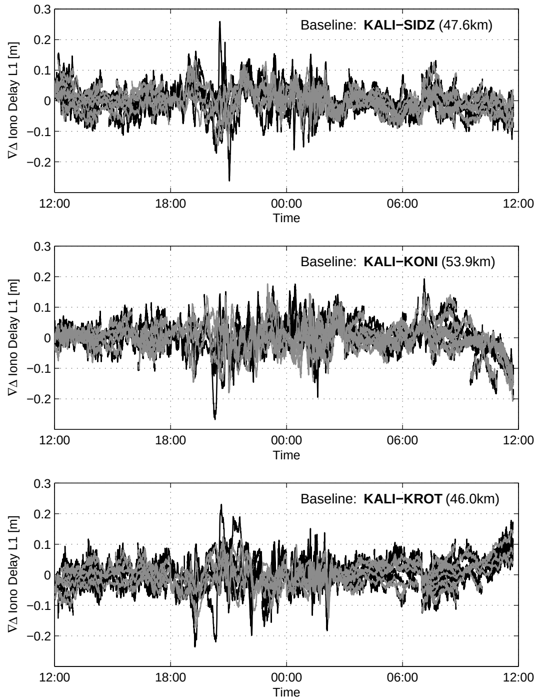

Figure 3. *Predicted using* WLIM *(*grey lines*) and real (*black lines*)* DD *ionospheric delay time series for user baselines*

cm and can significantly hinder the AR determination (see Landau *et al.*, 2003). The differences between predicted and real value of double-differences ionospheric delay were called *true ionospheric residuals* and were used in Section 3.3 to verify the ionospheric quality indicator performance.

3.2 Calculation of ionospheric mapping function

In this Section the algorithm of calculating the ionospheric elevation mapping function $\mu(\varepsilon)$ from the test network data, based on the formulas presented in Section 2.3, is described. The approach used here was proposed and described in details by Raquet (1998).

The ionospheric mapping function was determined on the basis of all combinations of double-differenced ionospheric delays from the 24-hour period. First, numerical estimates of $\mu(\varepsilon)$ were calculated for 55 baselines (it is the number of all baselines between all reference stations, except user stations, in the test network). For this purpose, the double-differenced ionospheric delays for which the minimum elevation of one of the satellites was above 45° were selected. Next, the selected delays were grouped into the 3° bins in according to the elevation of lower satellite from reference-other satellite pair. For each bin the variance of the ionospheric delay was computed using Equation 12. Equations 13 and 14 were used to calculate estimates of the mapping function for each bin with the assumption that ε^a denotes the low-elevation satellite and ε^b denotes the high-elevation satellite. The variance of zenith double-differenced ionospheric delays $\left(E[(\nabla\Delta I_{i,j}^{a,b} z)^2]\right)$ needed to solve the Equations 13 and 14, were found by extrapolating the variance of ionospheric delay to zenith. The elevation scaling factor for the high-elevation satellite $\mu\left(\varepsilon^b\right)$ was calculated for each bin using the average value of the nominal mapping function, from the Klobuchar ionospheric model (Klobuchar, 1987):

$$\mu(\varepsilon) = 1 + 16\left(0.53 - \frac{\varepsilon}{\pi}\right)^3 \tag{15}$$

over the 24-hour period.

Figure 4 shows the values of $\mu(\varepsilon)$ calculated for each of the elevation bin for all 55 baselines. At the end of the algorithm presented in this Section, the ionospheric elevation mapping function was determined, as follows:

$$\mu(\varepsilon) = \frac{1}{\sqrt{\sin\varepsilon}} + c_\mu\left(0.53 - \frac{\varepsilon}{\pi}\right)^3. \tag{16}$$

This function is a modification of the mapping function from the Klobuchar ionospheric model (see Equation 15) which provides a good fit for the estimated values. The parameter c_μ is the constant value calculated by least-squares fitting the function to data presented in Figure 4. In Figure 5 the ionospheric elevation mapping

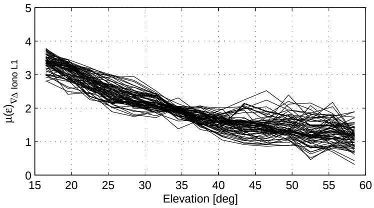

Figure 4. *Estimate of elevation mapping function for all baselines*

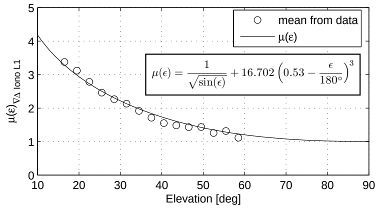

Figure 5. *Elevation mapping function for DD L1 ionospheric delay*

function was presented (the circle denotes the mean value of the mapping function estimation for all baselines).

3.3 Calculation of the ionospheric quality indicator

The ionospheric quality indicator described in this paper was determined as a standard deviation (σ_r) of a modeled double-differenced ionospheric delay using the WLIM method (see Equation 8). In order to compute a cumulative indicator for the all predicted double-differenced biases, the ionospheric elevation mapping function ($\mu(\varepsilon)$) was calculated (see Equation 16). The predicted errors were scaled to zenith. The proposed ionospheric quality indicator, called the Zenith Ionospheric Residual Interpolation Uncertainty, with a confidence level of 95%, can be described by the equation:

$$\mathrm{ZIRIU95} = 1.96\sqrt{\frac{1}{n}\sum_{i=1}^{n}\left(\frac{2\sigma_r^{ref,i}}{\mu\left(\varepsilon^{ref}\right)+\mu\left(\varepsilon^{i}\right)}\right)^2} \qquad (17)$$

where superscript denotes satellite (*ref* is the reference and i is the other satellite) and n is the number of double-differenced ionospheric observations. It should be noted that the proposed indicator is a modification of a similar indicator described by Chen *et al.* (2003).

A comparison of the results calculated for user baselines using ZIRIU95 method with the true zenith double-differenced ionospheric residual error scaled to zenith are presented in Figure 6. The true residual error was computed as a mean error of true ionospheric

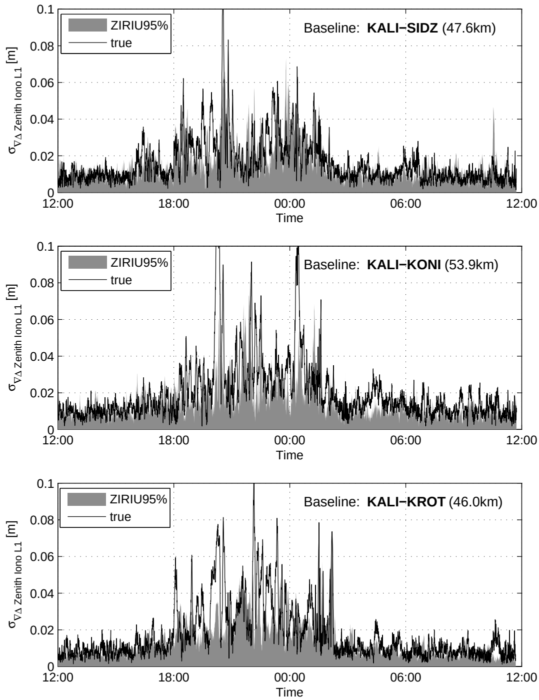

Figure 6. *True* DD *zenith ionospheric residuals (*solid lines*) and predicted* ZIRIU95 *(*shaded greys*) for the user baselines*

residuals (differences between predicted and real value). The quality indicator shows a very good agreement with the true errors for all three baselines. Only during the ionospheric storm (from 18 to 3 UT) can it be noted that true errors were more disturbed and slightly higher.

The ZIRIU95 value was also computed at certain epoch using a grid of rover position within the test network area. These values were used to generate the maps of ZIRIU95, which are shown in Figures 7 and 8 for two certain epochs. The map of ZIRIU95 generated for quite low ionospheric activity, when predicted residual zenith ionospheric error was less than 0.04 m, is shown in Figure 7. In Figure 8 the maximum predicted error reached 0.08 m and indicated the ionosphere disturbance. These maps give a quality

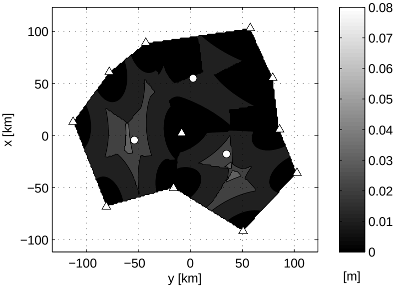

Figure 7. *ZIRIU95 (18:39:45 UT, 4.06.2011)*

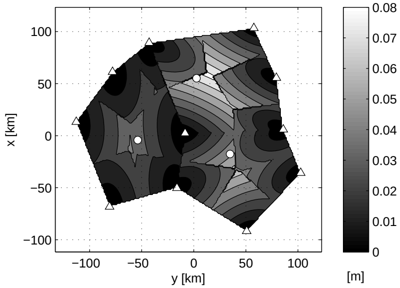

Figure 8. *ZIRIU95 (21:53:00 UT, 4.06.2011)*

assessment of remaining ionospheric biases and can be very helpful to evaluate the Network RTK performance.

4 Conclusions

In this paper the ionospheric quality indicator, called Zenith Ionospheric Residual Interpolation Uncertainty, was presented. This indicator describes remaining ionospheric errors after applying the correction terms obtained from an interpolation model. The performance of ZIRIU95 was tested using the test network and yielded very good agreement with the observed errors. The presented ZIRIU95 maps provide very useful information to predict the performance of Network RTK positioning. It should be noted that the described indicator can be accumulated over specified time interval (e.g. 1 hour) and a similar indicator can be computed for non-dispersive biases too.

References

Alves, P., I. Geisler, N. Brown, J. Wirth, H.-J. Euler (2005). Introduction of a geometry-based Network RTK quality indicator, *Proceedings of the 18th International Technical Meeting of the Satellite Division of the Institute of Navigation* ION GNSS 2005, 2552–2563.

Bartels, J. (1957). The technique of scaling indices K and Q of geomagnetic activity, *Annals of the International Geophysical Year* 4, 215–226.

Bosy, J., A. Oruba, W. Graszka, M. Leończyk, M. Ryczywolski (2008). ASG-EUPOS densification of EUREF Permanent Network on the territory of Poland, *Reports on Geodesy* 2(85), 105–112.

Chang, X., X. Yang, Z. T. (2005). MLAMBDA: A modified LAMBDA method for integer least-squares estimation, *Journal of Geodesy* 79, 552–565.

Chen, X., S. Han, C. Rizos, C. P. Goh (2000). Improving real time positioning efficiency using the Singapure integrated multiple reference station network (SIMRSN), *Proceedings of the 13th International Technical Meeting of the Satellite Division of the Institute of Navigation* ION GPS 2000, 9–16.

Chen, X., H. Landau, U. Vollath (2003). New tools for Network RTK integrity monitoring, *Proceedings of the 16th International Technical Meeting of the Satellite Division of the Institute of Navigation* ION GPS/GNSS 2003, 1355–1360.

Grejner-Brzezińska, D. A., I. Kashani, P. Wielgosz (2005). On accuracy and reliability of instantaneous network RTK as a function of network geometry, station separation, and data processing strategy, *GPS Solutions* 9(3), 212–225.

Hofmann-Wellenhof, B., H. Lichtenegger, E. Wasle (2008). *GNSS Global Navigation Satellite Systems: GPS, GLONASS, Galileo & more*, Springer, Wien, New York.

Klobuchar, J. (1987). Ionospheric time-delay algorithm for single-frequency GPS users, *IEEE Transactions on Aerospace and Electronic Systems* 23(3), 325–331.

Landau, H., U. Vollath, X. Chen (2003). Virtual reference stations versus broadcast solutions in network RTK–advantage and limitations, *Proceedings of the European Navigation Conference* GNSS2003.

Mader, G. (1999). GPS antenna calibration at national geodetic survey, *GPS Solutions* 3(1), 50–58.

Melbourne, W. G. (1985). The case for ranging in GPS based geodetic systems, *Proceedings of the 1st International Symposium on Precise Positioning with the Global Positioning Systems* pages 373–386.

Mervart, L. (1995). *Ambiguity resolution techniques in geodetic and geodynamic applications of Global Positioning Systems*, Ph.D. thesis, University of Berne.

Niell, A. E. (1996). Global mapping functions for the atmosphere delay at radio wavelengths, *Journal of Geophysical Research* 101(B2), 3227–3246.

Próchniewicz, D. (2011). A study on mitigation of the distance-dependent biases in the Network RTK Technique, *Reports on Geodesy* 1(90).

Raquet, J. (1998). *Development of a method for kinematic GPS carrier-phase ambiguity resolution using multiple reference receivers*, Ph.D. thesis, University of Calgary.

Rizos, C. (2002). Network RTK research and implementation – a geodetic perspective, *Journal of Global Positioning Systems* 1(2), 144–150.

Saastamoinen, J. (1973). Contributions to the theory of atmospheric refractions, *Bulletin Géodésique* 107(1), 13–34.

Teunissen, P. (1995). The least-squares ambiguity decorrelation adjustment: a method for fast GPS ambiguity estimation, *Journal of Geodesy* 70, 65–82.

Wanninger, L. (1995). Improved ambiguity resolution by regional differential modeling of the ionosphere, *Proceedings of the 8th International Technical Meeting of the Satellite Division of the Institute of Navigation* ION GPS 1995, 55–62.

Wanninger, L. (2004). Ionospheric disturbance indices for RTK and Network RTK positioning, *Proceedings of the 17th International Technical Meeting of the Satellite Division of the Institute of Navigation* ION GNSS 2004, 2849–2854.

Wübbena, G. (1985). Software Developments for Geodetic Positioning with GPS Using TI 4100 Code and Carrier Measurements, *Proceedings of the 1st International Symposium on Precise Positioning with the Global Positioning Systems* pages 403–412.

Wübbena, G., A. Bagge, G. Seeber, V. B oder, P. Hankemeier (1996). Reducing distance dependent errors for real-time precise DGPS applications by establishing reference station networks, *Proceedings of the 9th International Technical Meeting of the Satellite Division of the Institute of Navigation* ION GPS 1996, 1845–1852.